STED nanoscopy of the centrosome linker reveals a CEP68-organized, periodic rootletin network anchored to a C-Nap1 ring at centrioles

Rifka Vlijm[a,b,1], Xue Li[c,d,1], Marko Panic[c,d], Diana Rüthnick[c], Shoji Hata[c], Frank Herrmannsdörfer[e], Thomas Kuner[e], Mike Heilemann[e,f,g], Johann Engelhardt[a,b], Stefan W. Hell[a,b,h,2], and Elmar Schiebel[c,2]

[a]Department of Optical Nanoscopy, German Cancer Research Center (DKFZ), 69120 Heidelberg, Germany; [b]Department of Optical Nanoscopy, Max Planck Institute for Medical Research, 69120 Heidelberg, Germany; [c]Zentrum für Molekulare Biologie der Universität Heidelberg (ZMBH), DKFZ-ZMBH Allianz, Universität Heidelberg, 69120 Heidelberg, Germany; [d]Hartmut Hoffmann-Berling International Graduate School of Molecular and Cellular Biology, Universität Heidelberg, 69120 Heidelberg, Germany; [e]Department of Functional Neuroanatomy, Institute for Anatomy and Cell Biology, Universität Heidelberg, 69120 Heidelberg, Germany; [f]BioQuant, Universität Heidelberg, 69120 Heidelberg, Germany; [g]Institute of Physical and Theoretical Chemistry, Johann Wolfgang Goethe-University, 60438 Frankfurt, Germany; and [h]Department of NanoBiophotonics, Max Planck Institute for Biophysical Chemistry, 37077 Göttingen, Germany

Contributed by Stefan W. Hell, January 21, 2018 (sent for review September 25, 2017; reviewed by Laurence Pelletier and Jordan Raff)

The centrosome linker proteins C-Nap1, rootletin, and CEP68 connect the two centrosomes of a cell during interphase into one microtubule-organizing center. This coupling is important for cell migration, cilia formation, and timing of mitotic spindle formation. Very little is known about the structure of the centrosome linker. Here, we used stimulated emission depletion (STED) microscopy to show that each C-Nap1 ring at the proximal end of the two centrioles organizes a rootletin ring and, in addition, multiple rootletin/CEP68 fibers. Rootletin/CEP68 fibers originating from the two centrosomes form a web-like, interdigitating network, explaining the flexible nature of the centrosome linker. The rootletin/CEP68 filaments are repetitive and highly ordered. Staggered rootletin molecules (N-to-N and C-to-C) within the filaments are 75 nm apart. Rootletin binds CEP68 via its C-terminal spectrin repeat-containing region in 75-nm intervals. The N-to-C distance of two rootletin molecules is ∼35 to 40 nm, leading to an estimated minimal rootletin length of ∼110 nm. CEP68 is important in forming rootletin filaments that branch off centrioles and to modulate the thickness of rootletin fibers. Thus, the centrosome linker consists of a vast network of repeating rootletin units with C-Nap1 as ring organizer and CEP68 as filament modulator.

centrosome | centrosome linker | STED superresolution | rootletin | CEP68

The centrosome is the main microtubule-organizing center of animal cells. It consists of centrioles of nine triplet microtubules that are surrounded by the pericentriolar material (PCM) (1). Centrioles provide the duplication capability of centrosomes and have a scaffold function for the PCM. The PCM carries the microtubule-organization activity of centrosomes (2, 3). Human interphase cells contain two centrosomes that are joined together by the centrosome linker. The centrosome linker is an oligomeric proteinaceous structure that connects the two centrosomes of a cell together into one microtubule-organizing unit (4).

The centrosome linker is composed of the proteins C-Nap1 (encoded by *CEP250*), rootletin (*CROCC*), and CEP68 (5–7). Rootletin is a long, filamentous protein that has self-assembly properties (8, 9). It is also a component of the cilia rootlets that dock the basal body of cilia to the nuclear surface by binding to the nuclear envelope protein Nesprin1 (8, 10). Additional proteins, namely LRRC45 and centlein, have been implicated in linker formation; however, their role is less clear (11, 12). The centrosomal linker has to be resolved before or at the beginning of mitosis to allow formation of the mitotic spindle (13). The timing of linker disassembly in the cell cycle determines the requirement of the mitotic motor protein Eg5 in spindle formation and has an impact on the efficiency of mitotic chromosome segregation (14, 15). In addition, in cancer cells, the elevated cyclin B2 levels hyperactivate polo-like kinase (i.e., PLK1), leading to the accelerated dissolution of the centrosome linker and the appearance of lagging chromosomes (16). Furthermore, a defective centrosome linker in interphase cells impairs Golgi organization and cell migration and influences the cellular position of cilia (17, 18). Interestingly, a truncating mutation in *CEP250* (C-Nap1) affects centriole cohesion and is associated with Seckel-like syndrome in cattle, implicating a role of the centrosome linker during development (19).

Most studies to date have focused on identifying linker components, yet our understanding of the molecular architecture of the centrosome linker and the function of linker components remains rudimentary. In a simple model, rootletin has been described to connect the two centrosomes of an interphase cell by forming a linear filament between the C-Nap1 anchor at the proximal end of each mother centriole (20). Considering the importance of the centrosome linker for mitosis, cancer development, and cilia organization, it is crucial to understand its architecture and the role of linker proteins in its organization.

Significance

The integrity of the centrosome linker that joints both centrosomes of a cell into one microtubule-organizing unit plays important roles in cell organization, chromosome segregation, and cancer development. However, little is known about the structure of the linker. Here, we show by stimulated emission depletion microscopy that the centrosome linker consists of a vast network of repeating rootletin units with a C-Nap1 ring at centrioles as organizer and CEP68 as filament modulator. Rootletin filaments originating from the two centrosomes form a web-like, interdigitating filamentous network, explaining the flexible nature of the centrosome linker and the ability of the kinesin motor Eg5 to disrupt the linker function by force.

Author contributions: R.V., X.L., M.P., D.R., S.H., S.W.H., and E.S. designed research; R.V. and X.L. performed research; R.V., X.L., S.H., F.H., and J.E. contributed new reagents/analytic tools; R.V., X.L., D.R., S.H., F.H., T.K., M.H., J.E., S.W.H., and E.S. analyzed data; R.V. and J.E. built the STED microscope; R.V. performed STED imaging; R.V. analyzed STED data; X.L. performed cell biological experiments; X.L. prepared STED/STORM samples; D.R. and F.H. performed STORM analysis; F.H. built the STORM microscope; T.K., M.H., J.E., and S.W.H. contributed to overall image analysis and interpretation; and R.V., X.L., and E.S. wrote the paper.

Reviewers: L.P., Samuel Lunenfeld Research Institute; and J.R., University of Oxford.

The authors declare no conflict of interest.

[1]R.V. and X.L. contributed equally to this work.

[2]To whom correspondence may be addressed. Email: shell@gwdg.de or e.schiebel@zmbh.uni-heidelberg.de.

This article contains supporting information online at www.pnas.org/lookup/suppl/doi:10.1073/pnas.1716840115/-/DCSupplemental.

Published online February 20, 2018.

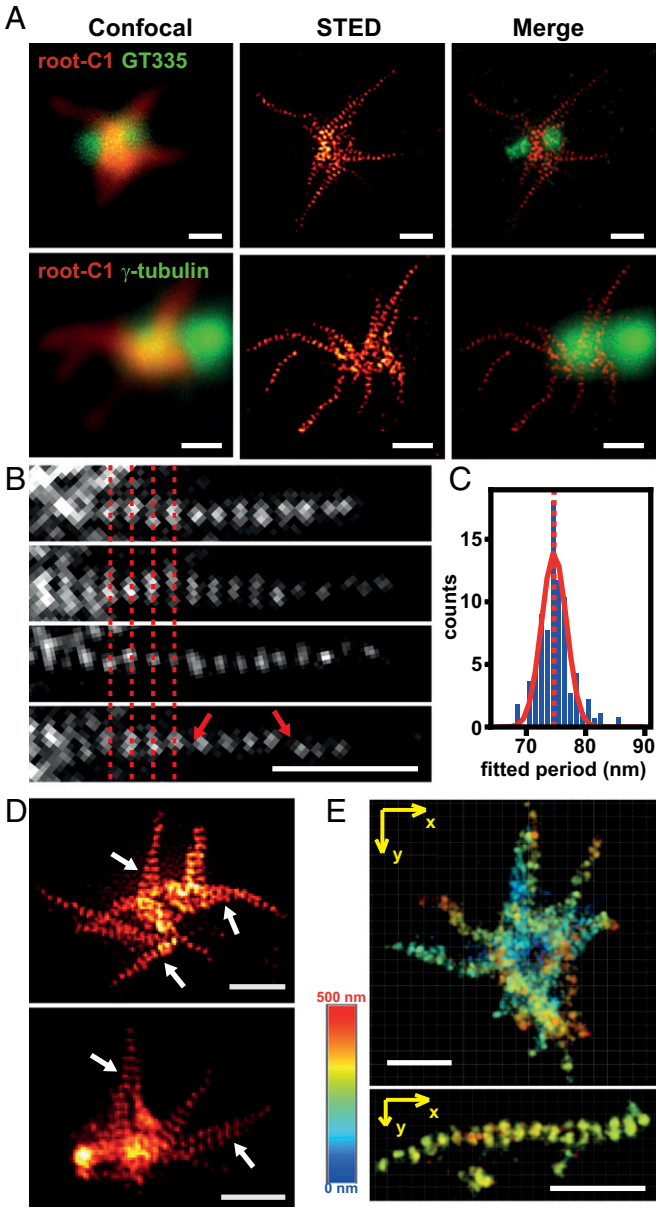

Fig. 1. Rootletin assembles into a web-like network with a repeat unit of 75 nm. (*A*) STED superresolution image of the rootletin linker (root-C1) of RPE-1 cells in combination with polyglutamylated tubulin (GT335, *Top*) or γ-tubulin (*Bottom*). (*B*) Single rootletin filaments from four different cells (red dotted lines 75 nm apart are a guide to the eye). Although the majority of rootletin spots are separated by 75 nm, a few locations show slightly different distances (red arrows). (*C*) Histogram of fitted periodicity. The Gauss fit (red line) gave a periodicity of 75 nm (red dotted line; SD, 2 nm). The data from three samples [47 cells; 112 line profiles with a total length of 79.48 μm (~1,060 periods)] were taken that could be fitted by using an automated procedure (*SI Appendix*, Fig. S2), with the length of the filament taken to weight. The maximum single fiber length is 2.5 μm. (*D*) Rootletin filaments are often thicker close to centrioles and taper off toward the tip (white arrows, *Top*). In some cases, these tapered filaments appear to be one fiber; in other cases, multiple fibers come together and align their periodicity (white arrows, *Bottom*). (*E*) Color-coded 3D rootletin (root-C2) network analyzed by 3D-STORM. The upper image shows the rootletin network (Movie S7). The lower image shows a single rootletin fiber (Movie S8). (All scale bars, 500 nm.) The STED images are Wiener deconvolved; the raw data are shown in *SI Appendix*, Fig. S11.

Here, we have analyzed the centrosome linker proteins C-Nap1, rootletin, and CEP68 by stimulated emission depletion (STED) microscopy (21–23), and direct 3D stochastic optical reconstruction microscopy (STORM) (24–26). Rootletin/CEP68 filaments form an extended, web-like network that spreads up to 1 to 2 μm outward from the C-Nap1 ring at the proximal end of both centrioles. Rootletin filaments coming from opposite centrioles are weaved into each other, which probably is the basis of centrosome linkage. STED-based statistical analysis showed that rootletin forms regular filaments, with a repeat organization of 75 nm (N-to-N or C-to-C). The N-to-C-distance of two rootletin molecules was measured to be ~35 to 40 nm, which leads to an estimated minimal rootletin length of ~110 nm. CEP68 binds to rootletin filaments every 75 nm via its C-terminal end that contains a conserved spectrin repeat. CEP68 affects the thickness of rootletin filaments and promotes filament formation from the rootletin ring that encircles C-Nap1 at centrioles. Based on these data, we suggest a model for the centrosome linker formation.

Results

The Centrosome Linker Is a Flexible Entity. Nontransformed human telomerase-immortalized retinal pigmented epithelial (RPE)-1 cells have a robust centrosome linker and are, therefore, ideally suited for the analysis of this structure by microscopy (17). Live-cell imaging analysis of RPE-1 FRT/T-Rex mNeonGreen-CEP68-P2A-mRuby2-PACT cells revealed that the two centrosomes in most cells were kept close together (<2 μm) during interphase (Movies S1–S3). However, in about 5% of the cells, both centrosomes moved several micrometers (>2 μm) apart. In many cases, this centrosome distance was >5 μm, exceeding the length of the centrosome linker (Movies S4–S6). Eventually, the centrosomes joined together and reestablished a functional centrosome linker, as indicated by the closeness of the two centrosomes over at least 20 min (Movies S4–S6). These data indicate that some cells lose centrosome linker function in a reversible manner, suggesting that the centrosome linker is a flexible structure.

CEP68 and Rootletin Form an Extended, Colocalizing Filamentous Network with a Repeat Organization of 75 nm. To understand the architecture of the centrosome linker, we localized the proteins rootletin and CEP68 in the centrosome linker by STED microscopy (5, 6). Analysis of rootletin with regional antibodies directed against the C terminus of the protein (named root-C1) and of CEP68 with a polyclonal antibody (*SI Appendix*, Fig. S1 *A–D*) detected both proteins as web-like filamentous networks that originated at each of the two centrioles marked by polyglutamylated tubulin, γ-tubulin, or C-Nap1 (Figs. 1*A* and 2*A*). Each centriole was associated with several rootletin and CEP68 filaments that radiated outward from the centriole into the cytoplasm.

STED images showed striated patterns for root-C1 and CEP68 fibers, indicating a highly ordered organization of both proteins in the filaments (Figs. 1 *A* and *B* and 2 *A* and *B*). Statistical analysis revealed a repeat organization of root-C1 and CEP68 of 75 nm along the filaments (Figs. 1*C* and 2*C* and *SI Appendix*, Fig. S2). The periodicity was independent of the filament length (*SI Appendix*, Fig. S2 *E* and *F*); however, it was disrupted in some regional cases, and then followed the 75-nm repeat interval again (Figs. 1*B* and 2*B*; red arrows). The length of rootletin and CEP68 filaments varied strongly. Most filaments were a few hundred nanometers long, but lengths just over 2 μm were also found (*SI Appendix*, Fig. S2 *E* and *F*). Filaments were often thicker close to centrioles and tapered off toward the tip (Figs. 1*D* and 2*D*). In some cases, these tapered filaments appeared to be one fiber; in other cases, multiple fibers came together and aligned their periodicity (Figs. 1*D* and 2*D*; white arrows).

We used nonsynchronized RPE-1 cells for analysis of the centrosome linker. About >80% of these RPE-1 cells are in G1 and S phases. To exclude that rootletin images were influenced by the dissolution of the linker in G2/M (4), we analyzed the root-C1 pattern in cells that were stained for the cell cycle

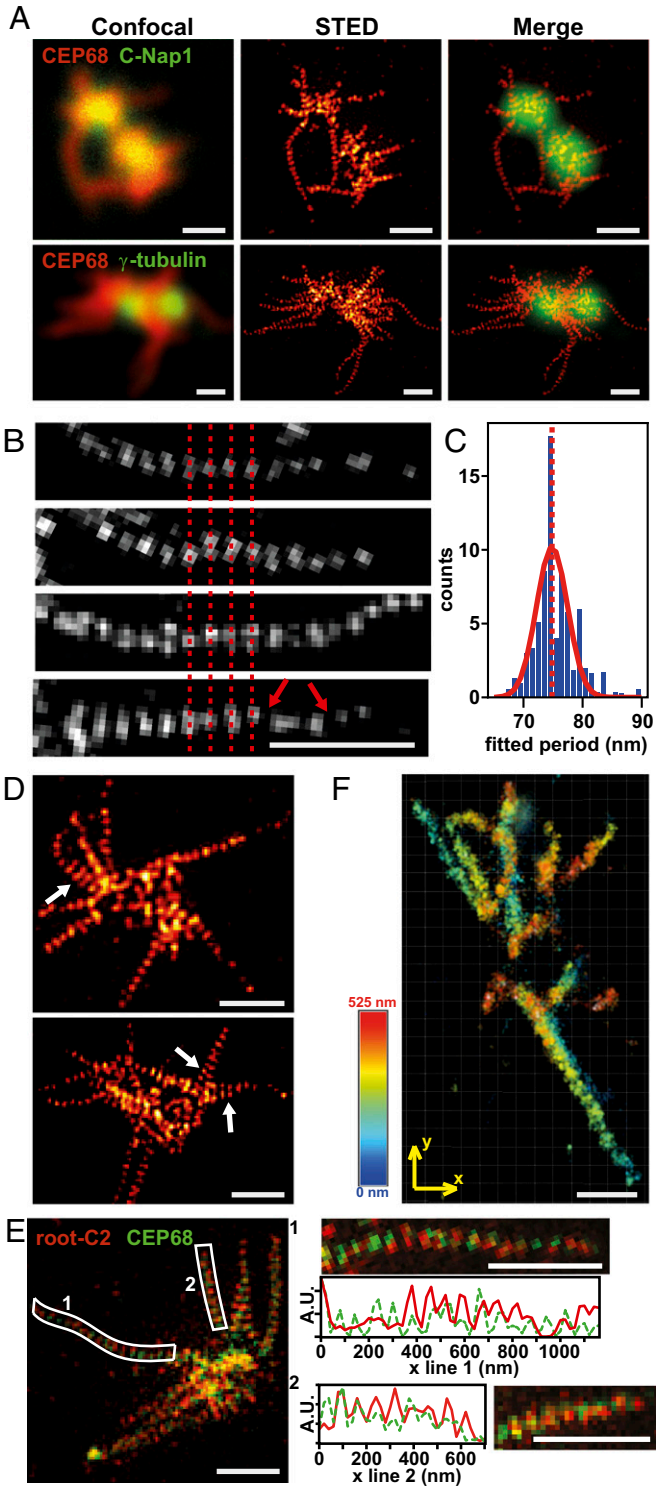

Fig. 2. Cep68 binds to rootletin filaments in 75-nm intervals. (*A*) STED images of CEP68 together with C-Nap1 (*Top*) or γ-tubulin (*Bottom*). (*B*) Single CEP68 filaments from the cell in *A* and three other cells (red dotted lines 75 nm apart are a guide to the eye). Although the majority of the CEP68 spots are separated by 75 nm, a few locations show slightly different distances (red arrows). (*C*) Histogram of fitted periodicity. CEP68 shows a regular 75 ± 3 nm repeat organization [three samples, plus one data point from a fourth sample; 38 cells; 142 line profiles; total length, 37.54 μm (~984 periods); maximum single fiber length, 1.34 μm]. (*D*) CEP68 filaments show thick to thin filaments (white arrow, *Top*), and even separate filaments synchronize their phase (white arrows, *Bottom*). (*E*) Rootletin (red) and CEP68 (green) colocalize along the same fiber [*Left*, STED; *Right*, intensity line profile and the filament (no. 1 or 2) it is taken from]. (*F*) Color-coded 3D CEP68 network of the cell shown in Movie S9 analyzed by 3D-STORM. (All scale bars, 500 nm.) The STED images are Wiener deconvolved; the raw data are shown in *SI Appendix*, Fig. S11.

marker CENP-F. CENP-F does not stain the nucleus in G1- and S-phase cells; however, it decorates the nuclear envelope and associates with kinetochores starting in G2 (27). Analysis of interphase cells lacking a nuclear CENP-F signal resulted in the same rootletin pattern as what was observed for CENP-F–positive interphase cells (*SI Appendix*, Fig. S3 *A* and *B*). Thus, the rootletin organization shown in Fig. 1 reflects the G1, S, and early G2 organization of the centrosome linker.

The very similar localization pattern of rootletin and CEP68 along centrosome linker filaments suggested that both proteins colocalize on the fibers. Indeed, the root-C1 and CEP68 signals localized dot-like along the same fibers in STED microscopy (Fig. 2*E*). Line profiling of the signal intensities showed near colocalization of the peak intensities in most cases (Fig. 2*E*, *Right*). Thus, CEP68 and the C terminus of rootletin localize close together on the filaments.

Lack of antibody accessibility to some epitopes could cause the striated C-rootletin staining pattern. To exclude this possibility, we measured localization of the N terminus of rootletin with a regional antibody root-N. Also, the root-N antibody resulted in a 75-nm periodic signal along the rootletin fiber (Fig. 3 *A*–*C*). We next analyzed localization of N- and C-terminal regions of rootletin within fibers. For this analysis, we used a second C-regional rootletin antibody (root-C2; *SI Appendix*, Fig. S1*A*) in combination with root-N. Root-C2 resulted in the same 75-nm periodicity as root-C1 (compare Fig. 1*C* with Fig. 3*C*). The root-N and root-C2 signals showed an average phase shift of 40 ± 7 nm (Fig. 3*D*) independent of the orientation of the filaments in the microscope (*SI Appendix*, Fig. S4 *A*–*D*). This result indicates a staggered overlap between rootletin molecules in the filaments and a minimal rootletin length of 110 nm (Fig. 3*E*). Considering the amino acid uncertainty of root-N and root-C2 binding, the distance between the N terminus and C terminus of one rootletin molecule may be even larger (*SI Appendix*, Fig. S4*D*).

The 3D network of rootletin and CEP68 in RPE-1 cells was further analyzed by 3D-STORM (Figs. 1*E* and 2*F* and Movies S7–S9). This confirmed the repeat structure of the filaments and the web-like organization of the network. Rootletin filaments that were organized by the two centrioles were weaved into each other. Regional contacts are probably the basis of centrosome linkage.

Rootletin Filaments Have a Similar Periodicity in Human Primary and Cancer Cells. To understand whether the highly organized centrosome linker of RPE-1 cells is a common feature in other cell types, we imaged rootletin and CEP68 localization by STED microscopy in RPE-1, primary human umbilical vein endothelial cells (HUVECs), and HCT116 colon cancer cells in relationship to the centrosomal marker γ-tubulin. The 75-nm repeat unit organization of rootletin and CEP68 was observed in all cell types (*SI Appendix*, Fig. S5). However, in HCT116 cells, the rootletin/CEP68 fibers were, in general, shorter and denser around the centrosomes and therefore more difficult to be resolved than in RPE-1 and HUVECs. Thus, the centrosome linker is a well-organized repeat structure, a feature that is common to human primary cells, telomerase-immortalized RPE-1 cells, and cancer cells.

C-Nap1 Forms a Ring at the Proximal End of Centrioles That Organizes CEP68 and Rootletin into Rings and Filaments. C-Nap1 is the anchor of the centrosome linker at the proximal end of centrioles (5). It

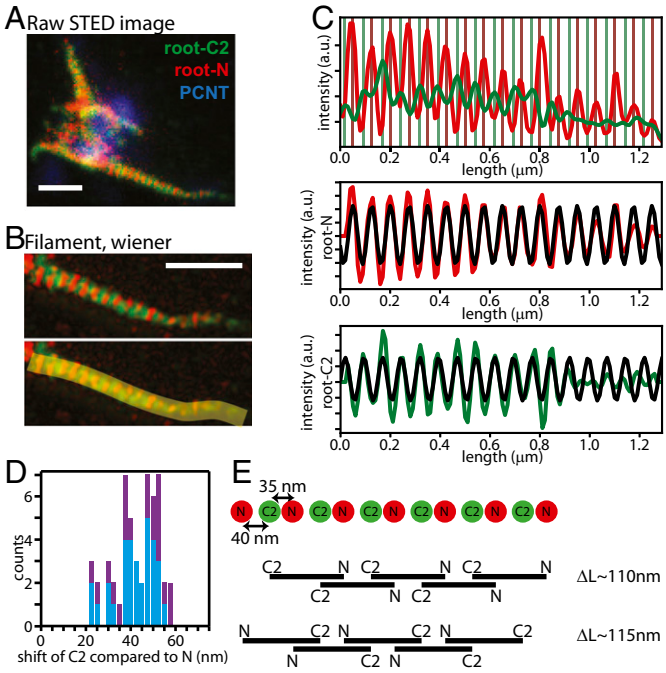

Fig. 3. Rootletin N-terminus and C-terminus localization along the fiber. (*A*) Raw-data STED image of the N- and C-terminus staining by root-N (red) and root-C2 (green) antibodies, respectively. Through confocal microscopy, PCNT (blue) is also imaged. (Scale bar, 500 nm.) (*B*) A deconvolved (Wiener) filament of the cell in *A* is shown, from which a line profile is drawn from centriole outward, as illustrated by the marked yellow area. (Scale bar, 500 nm.) (*C*) The line profiles show that both root-N and root-C2 give a 75-nm periodic signal along the fiber. The shift in phase of root-C2 compared with root-N (drawn from the centriole outward) is 43 nm, as indicated by the red and green lines at the peaks. (*D*) Histogram of the shift of the root-C2 signal compared with the root-N signal (26 cells; 48 line profiles with a total length of 43.6 μm). The root-C2 signal is, on average, shifted by 40 ± 7 nm compared with the root-N signal (as measured from the centriole outward). Blue data are from root-N to the kk114L dye and root-C2 to the star580 dye, and the purple data are from the reversed staining. (*E*) The results indicate an overlap between individual rootletin molecules, as drawn. More examples in other directions and with reversed staining are given in *SI Appendix*, Fig. S4, and the raw and Wiener deconvolved images are shown in *SI Appendix*, Fig. S11.

has been suggested that rootletin and CEP68 localization with centrioles depends on C-Nap1 (6, 7). We confirmed these data by using a *CEP250* (C-Nap1) knockout (KO) cell line and siRNA depletion of C-Nap1 (*SI Appendix*, Fig. S6 *A* and *B*) (17). Consistent with published data (6), siRNA depletion of C-Nap1 can result in centrioles carrying only one or very few elongated rootletin fibers (*SI Appendix*, Fig. S6*B*), probably because of a minor residual pool of C-Nap1 at centrosomes despite efficient depletion (*SI Appendix*, Fig. S1 *E* and *F*). Interestingly, ∼10 to 20% of *CEP250* (C-Nap1) KO cells contained rootletin filaments in the cytoplasm, with no connection to the γ-tubulin–marked centrosome (*SI Appendix*, Fig. S6 *C* and *D*). A similar frequency of free-floating rootletin filaments was observed in RPE-1 wild-type cells (*SI Appendix*, Fig. S6*D*). siRNA depletion of C-Nap1 did not significantly affect the number of free rootletin filaments of RPE-1 cells (*SI Appendix*, Fig. S6*D*). These data indicate that C-Nap1 is not essential for rootletin filament assembly. However, in wild-type cells, C-Nap1 organizes the centriole-associated rootletin network.

To understand the function of C-Nap1 as organizer of rootletin/CEP68 filaments, we determined the structure of C-Nap1 with a regional antibody (*SI Appendix*, Fig. S1*E*) directed against the C terminus relative to CEP68 by dual-color STED microscopy. The C-Nap1 signal was resolved as a ringlike structure with an average diameter of 265 ± 35 nm (n = 55, from 34 individual cells) that was surrounded by a wider CEP68 ring (Fig. 4*A*; note that in *Top*, C-Nap1 was imaged first; in *Middle* and *Bottom*, CEP68 was imaged first). Dual-color STED microscopy showed CEP68 and rootletin rings with attached filaments (Fig. 4*B*). Each filament originated from a thicker anchoring point at the rootletin/CEP68 ring. The outcome of this analysis suggests that C-Nap1 at centrioles functions as organizer of rootletin and CEP68 rings. These rings are then the anchoring point of rootletin/CEP68 filaments that radiate into the cytoplasm.

The Rootletin Ring on Top of C-Nap1 Is Less Sensitive to CEP68 Depletion than Filaments. To find further support for rootletin/CEP68 rings that are organized by the C-Nap1 ring and to understand the function of the individual proteins in this organization, we tested how modulation of CEP68, rootletin, and C-Nap1 affected rootletin/CEP68 rings and filaments. Depletion of CEP68 (*SI Appendix*, Fig. S1*C*) removed most of the rootletin signal from centrioles in comparison with the nonspecific control (NSC) (*SI Appendix*, Fig. S7 *A* and *B*) (7, 12). Analysis of the

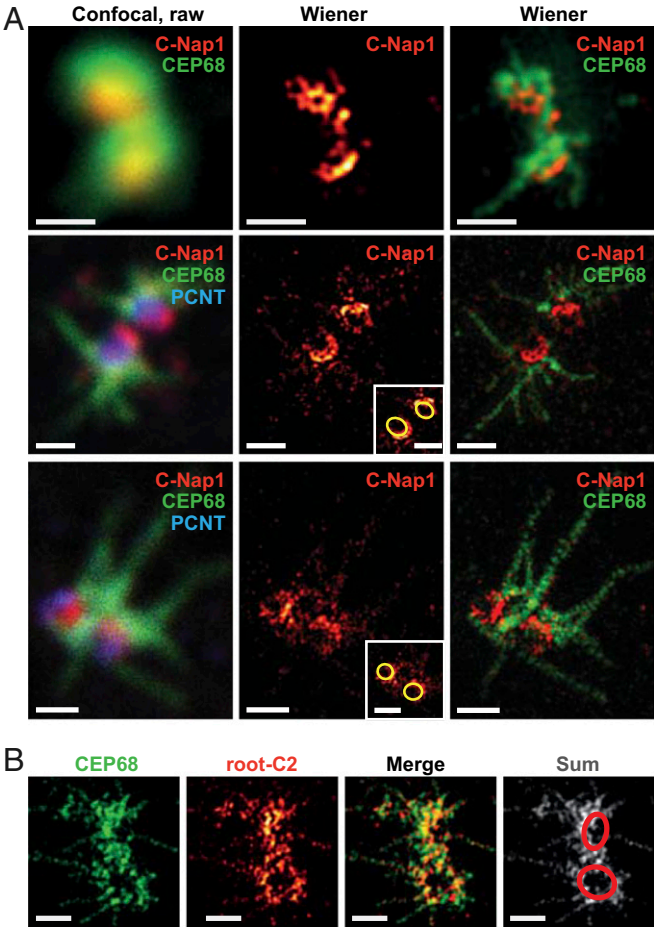

Fig. 4. C-Nap1 forms a ring at centrioles and functions as rootletin filament organizer. (*A*) Three examples of dual-color STED analysis of C-Nap1 [monoclonal anti-C-Nap1 mouse antibody (34)] labeled with kk114L and of CEP68 (polyclonal anti-rabbit antibody) labeled with star600 (*Top*) and star580 (*Middle* and *Bottom*). (*Top*) For optimal imaging of the C-Nap1 ring, C-Nap1 was imaged first, followed by CEP68, in each scanned line. (*Middle* and *Bottom*) The imaging order in *Top* was reversed to increase the resolution of the CEP68. The C-Nap1 ring is illustrated in the *Middle* and *Bottom Insets*. (*B*) Dual-color STED analysis of CEP68 and rootletin shows ringlike colocalization of both proteins. (Scale bars, 500 nm.) The STED images are Wiener deconvolved; the raw data are shown in *SI Appendix*, Fig. S11.

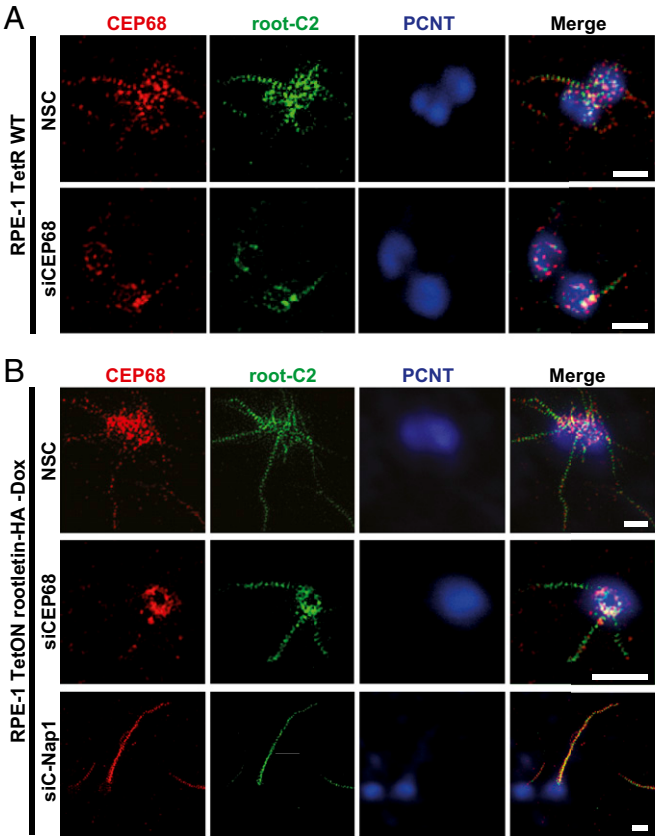

Fig. 5. STED analysis of centriolar rootletin/CEP68 structures. PCNT in confocal imaging was used as a marker for centrioles. (*A*) Rings and often a single filament of rootletin and residual CEP68 at PCNT-marked centrosomes in response to siRNA CEP68 depletion. The NSC siRNA control is shown as comparison. (*B*) Mild overexpression of *CROCC* (rootletin) in combination with siRNA depletion of CEP68 or C-Nap1 in the absence of Dox. siRNA depletion of CEP68 in *CROCC* (rootletin)-overexpressing cells exposes a strong centriole rootletin/CEP68 ring. C-Nap1 is essential for centriolar rootletin/CEP68 ring assembly, even when *CROCC* (rootletin) is overexpressed. A single or very few elongated rootletin/CEP68 filaments that originate at centrosomes were observed in siC-Nap1-depleted cells. (Scale bars, 500 nm.) More examples are shown in *SI Appendix*, Fig. S8*C*. The STED images are Wiener deconvolved; the raw data are shown in *SI Appendix*, Fig. S11.

CEP68-depleted cells by STED microscopy revealed rings of rootletin and residual CEP68 at pericentrin (PCNT)-marked centrosomes (Fig. 5*A*, *Bottom*; see *SI Appendix*, Fig. S8*A* for more examples; and see *SI Appendix*, Fig. S11 for "raw" images). CEP68 depletion resulted in a lower number of rootletin filaments per centrosome without strongly affecting the rootletin ring surrounding the centriole (compare NSC with siCEP68 in Fig. 5*A* and *SI Appendix*, Fig. S8*A*). In about half of the cells, one or two rootletin filaments were visible that were anchored to the centriolar ring by intense, colocalizing CEP68 and rootletin dots (Fig. 5*A*, *Bottom*). Thus, rings and filaments of rootletin have different CEP68 requirements.

We modulated the rootletin/CEP68 system by overexpression of the *CROCC* gene coding for rootletin with or without depletion of CEP68 or C-Nap1. Mild overexpression of *CROCC* (rootletin) due to the leakiness of the TetON promoter [*SI Appendix*, Fig. S1*I*, absence of doxycycline (−Dox)] enhanced the rootletin/CEP68 filament network at centrosomes (Fig. 5*B*, NSC; Fig. 6*A*; *SI Appendix*, Fig. S8*B*, NSC; and *SI Appendix*, Fig. S9*A*). In some TetON-*CROCC* (rootletin) cells, the rootletin/CEP68 network surrounding centrosomes was so dense that it was difficult to identify the individual filaments (*SI Appendix*, Fig. S8*B*, fourth cell). When, in addition, CEP68 levels were reduced, the number of centriolar rootletin/CEP68 filaments declined, revealing a pronounced rootletin/CEP68 ring at centrosomes (Fig. 5*B*, siCEP68 and *SI Appendix*, Fig. S8*B*). Even under *CROCC* (rootletin) mild overexpression conditions, depletion of C-Nap1 strongly affected CEP68 and rootletin at centrioles, confirming the absolute requirement of C-Nap1 for rootletin/CEP68 centriolar ring assembly (Fig. 5*B*, siC-Nap1 and *SI Appendix*, Fig. S8*C*). In some C-Nap1–depleted cells, a small number of rootletin/CEP68 fibers up to 5-μm long originated from centrosomes, probably because C-Nap1 depletion at centrosomes was incomplete. These data confirm that the organization of CEP68 and rootletin rings at centrioles is dependent on C-Nap1.

CEP68 Bundles Rootletin Filaments. Mild overexpression of HA-tagged *CROCC* (rootletin-HA) (*SI Appendix*, Fig. S1*I*, −Dox, long exposure) extended the rootletin/CEP68 network at centrosomes (for an example, see *SI Appendix*, Fig. S9*A*). However, it also increased the number of cells with cytoplasmic rootletin filaments that were not associated with centrosomes from ∼10 to 30% to nearly 100% [compare *SI Appendix*, Fig. S6*D*, i.e., endogenous, with Fig. 6*D*, i.e., mild *CROCC* (rootletin) overexpression]. Mild *CROCC* (rootletin)-overexpressing cells contained thin and thick, noncentrosome-associated rootletin filaments (Fig. 6*A*). Thick rootletin filaments (Fig. 6*A*, arrowheads) were associated with CEP68, while thin filaments, which became visible in the high brightness and contrast ("high") image, were mostly devoid of CEP68 (Fig. 6*A*, asterisks). STED analysis confirmed that thicker rootletin filaments as seen by confocal microscopy were decorated by CEP68 (Fig. 6*B*, *Bottom*). To thin rootletin fibers, CEP68 was either not, or only sparsely, associated (Fig. 6*B*, *Right* and *SI Appendix*, Fig. S9*A*, *Bottom*). This suggests that thin rootletin filaments can assemble without the aid of CEP68.

Importantly, siRNA depletion of CEP68 reduced the number of thick rootletin bundles in TetON-*CROCC* (rootletin) cells (Fig. 6 *C* and *D*). This was particularly obvious in the low brightness and contrast ("low") image of siCEP68-depleted cells. In contrast to the NSC cells that showed thick rootletin filaments in the low image (Fig. 6*C*, *Top*), the only detectable rootletin signal of siCEP68 cells in the low image was associated with PCNT at centrosomes. However, the high image of siCEP68 cells detected a network of rootletin fibers at the nucleus (Fig. 6*C*). The nuclear association possibly reflects the affinity of the nuclear envelope protein Nesprin1 for rootletin (10). STED analysis resolved these rootletin fibers of siCEP68 cells as thin rootletin filaments that lacked a CEP68 signal (*SI Appendix*, Fig. S9*B*, *Bottom*). These data suggest that CEP68 plays a role in bundling thin rootletin filaments into thicker filaments. Consistent with this notion is the finding that co-overexpression of both *CEP68* and *CROCC* (rootletin) promoted the assembly of an extended, dense rootletin/CEP68 network that hardly allowed resolving individual rootletin filaments (*SI Appendix*, Fig. S8*D*).

The C-Terminal Globular Domain of CEP68 Containing the Spectrin Repeat Interacts with Centrosomes. The regular interaction pattern of CEP68 with rootletin fibers indicates a defined binding site in CEP68 that interacts with a specific region in rootletin. Recently, Nesprin1 was described as a rootletin binding partner (10). We compared both proteins for homology. Interestingly, CEP68 carries one spectrin repeat sequence at the C terminus of the protein (Fig. 7*A*). Several of these spectrin repeats are present in Nesprin1 (10).

To test whether the spectrin repeat of CEP68 has a role in rootletin binding, we expressed, full-length, the N-terminal fragments (amino acids 1 to 298) and C-terminal fragments (amino acids 618 to 757) of CEP68 in RPE-1 cells (*SI Appendix*,

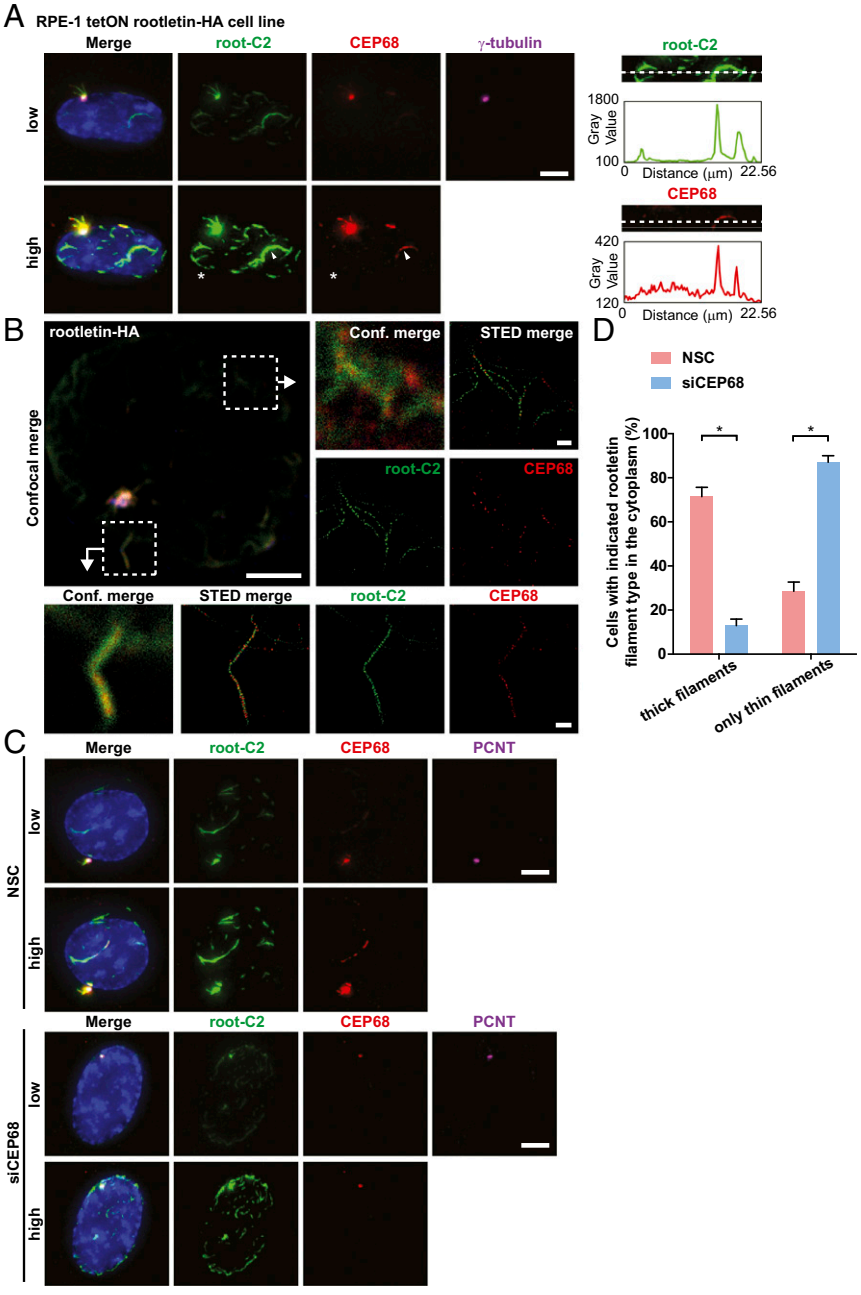

Fig. 6. CEP68 plays a role in rootletin filament bundling. (*A*) In the RPE-1 TetON rootletin-HA cell line, mild overexpression of *CROCC* (rootletin) promotes assembly of thin and tick rootletin filaments. Only thick filaments were associated with CEP68 (arrowheads). Thin filaments (asterisks) were mostly devoid of CEP68. Low and high images reflect different contrast and brightness settings of the same image. Note that thin filaments were detected only with the higher sensitivity of the high setting. The line scan (*Right*) indicates colocalization of CEP68 and rootletin (stained with root-C2) on thick filaments. (*B*) Analysis of rootletin filaments of cells from *A* for CEP68 and rootletin by confocal microscopy and dual-color STED microscopy. The smaller images at the *Right* and *Bottom* show enlargements of thin and thick rootletin filaments, respectively. The STED images are Wiener deconvolved; the raw data are shown in *SI Appendix*, Fig. S11. (*C*) siRNA depletion of CEP68 in RPE-1 TetON rootletin-HA cells decreases the number of cells with cytosolic rootletin thick filaments. Instead, thin rootletin filaments encircle the nuclear envelope. These thin filaments were more visible with the high setting. They were resolved as single rootletin filaments by STED microscopy (*SI Appendix*, Fig. S9*B*). (*D*) Quantification of *C*: $n = 3$; $n \geq 20$; mean and SD are shown. (*A* and *C* scale bars, 5 μm; *B* scale bars, 500 nm.)

Fig. S1 *J* and *K*). The C-terminal fragment containing the spectrin repeat bound to centrioles, as was the case for full-length CEP68 (Fig. 7*B*). In contrast, the N-terminal CEP68 fragment was diffusely distributed in cells (*SI Appendix*, Fig. S10*A*). Because CEP68 binding to centrosomes requires rootletin (7, 12), these data suggest that the C terminus of CEP68 with the spectrin repeat interacts with centrosomes via rootletin.

To identify rootletin fragments that interact with CEP68, we used a published assay based on the overexpression of rootletin subfragments that form cytoplasmic filaments or larger protein assemblies (*SI Appendix*, Fig. S1 *G–I*) (7, 9). We asked whether fragments of rootletin recruit endogenous CEP68 as an indication for interaction. Interestingly, the overexpressed rootletin R3 subfragment (amino acids 1,079 to 1,825) recruited endogenous CEP68 (Fig. 7*C*, enlargement on right and Fig. 7*D*). Fragment R2 was expressed in RPE-1 cells (*SI Appendix*, Fig. S1*G*); however, it did not show formation of dense assemblies (*SI Appendix*, Fig. S10*B*). R1 and R4 formed cytoplasmic assemblies or filaments that did not recruit CEP68 (Fig. 7 *C* and *D*). The larger R123 and R234 rootletin fragments containing R3 recruited CEP68 (Fig. 7 *C* and *D*). CEP68 recruitment by R3 suggests interaction of CEP68 with this region of rootletin.

Discussion

The centrosome linker has essential functions in connecting both centrosomes of an interphase cell into one microtubule-organizing unit. Failure of this organization has profound consequences for cell organization, cell migration, cilia formation, and chromosome segregation in mitosis (16–18). Despite these important functions, relatively little is known about the structure of the centrosome linker. Rootletin, a linker protein, is also a component of the cilia rootlets. Rootletin fibers in cilia rootlets

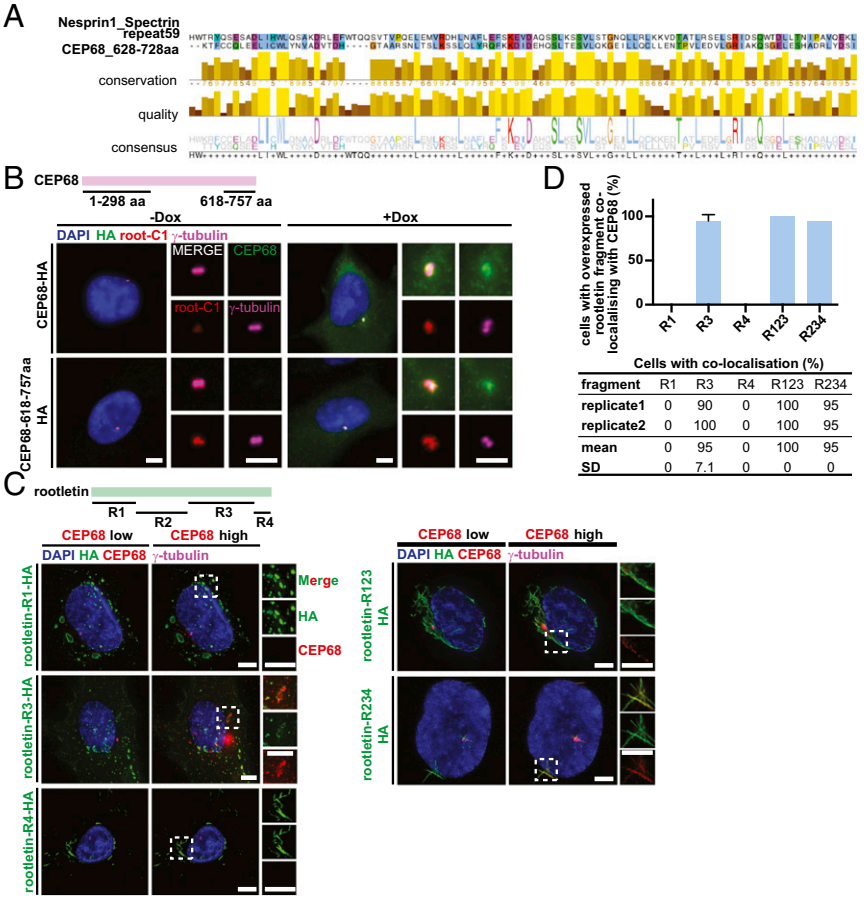

Cells with co-localisation (%)

fragment	R1	R3	R4	R123	R234
replicate1	0	90	0	100	95
replicate2	0	100	0	100	95
mean	0	95	0	100	95
SD	0	7.1	0	0	0

Fig. 7. The C terminus of CEP68 containing the spectrin repeat mediates binding to centrosomes. (*A*) The C terminus of CEP68 contains a spectrin repeat. Sequence alignment of CEP68 with Nesprin1 identified a spectrin repeat in the CEP68 C terminus (amino acids 628 to 728). (*B*) The C-terminal CEP68 fragment (amino acids 618 to 757) localizes to the centrosome, as does CEP68. Shown are stable RPE-1 TetON CEP68-HA cells with Dox (+Dox) or without (−Dox). Root-C1 antibody was used to stain rootletin. γ-Tubulin was used as marker for centrosomes. The smaller images to the *Right* of each cell are enlargements of the centrosomal area and indicate CEP68-618–757aa-HA recruitment to centrosomes upon Dox induction (+Dox). CEP68-HA was used as a positive control. In contrast, the N-terminal CEP68 fragment (amino acids 1 to 298) shows no defined localization (*SI Appendix*, Fig. S10*A*). (*C*) The rootletin fragment R3 recruits CEP68. Cells with expression of the HA-tagged *CROCC* (rootletin) constructs in stable RPE-1 TetON cell lines. Antibodies against HA, CEP68, and γ-tubulin were used. DNA was stained with DAPI. Low (*Left*) and high (*Center*) images reflect different contrast and brightness settings of the same CEP68 image. (*Right*) Enlargement(s) of the boxed area in the image to the left. CEP68 localization in cells expressing R2 is shown in *SI Appendix*, Fig. S10*C*. (*D*) Quantification of *C*: $n = 2$; $n = 20$; mean and SD are shown. (*B* and *C* scale bars, 5 μm.)

have a repeat organization of 60 to 70 nm as seen by electron microscopy (8, 9). Puzzlingly, however, ordered filaments have not been observed in between the two centrosomes by electron microscopy (6), raising the possibility that rootletin in the centrosome linker has a fundamentally different organization than in cilia rootlets.

To solve this riddle, we turned to STED microscopy and 3D-STORM. Superresolution microscopy has paved the way before in centrosome biology by showing that the interphase PCM is an ordered array of proteins that surround centrioles (3, 28, 29). A striking feature of the rootletin filaments as resolved by STED microscopy is the 75-nm periodic organization of the N terminus and C terminus of rootletin. This repeat organization suggests that rootletin also assembles in an ordered manner in the centrosome linker and is most easily explained by an N- and C-terminal overlap of two elongated rootletin molecules (Fig. 8*A*). The N-to-C distance of two rootletin molecules along the filament is in the range of ∼35 to 40 nm as determined by dual-color STED microscopy with N- and C-specific rootletin antibodies (root-N and root-C2, respectively) (Fig. 3 and *SI Appendix*, Fig. S4). Repeating this interaction will result in a protofilament with defined spacing of rootletin N and C termini. Based on our measurements, rootletin has a minimal length of ∼110 nm (Fig. 3). However, it may be an even more extended molecule (up to 160 nm), depending on the precise position of the antibody binding sites (*SI Appendix*, Fig. S4*D*).

CEP68 follows the C-rootletin order because it binds to the R3 region of rootletin. R3 neighbors the C terminus of rootletin (Figs. 7*C* and 8*A*). This closeness is consistent with the near colocalization of the CEP68 and root-C2 signals along fibers as shown by STED microscopy. CEP68 binding to rootletin increases the thickness of rootletin fibers. Presently, it is unclear how CEP68 interconnects thinner rootletin filaments.

Interestingly, the C-terminal fragment of CEP68 that interacts with rootletin contains a spectrin repeat. Also, Nesprin1 that interacts with rootletin in rootlets harbors spectrin repeats (10). Spectrin repeats are platforms for cytoskeletal protein assemblies (30). We propose that certain spectrin repeats have the ability to interact with rootletin filaments. Additional experiments are needed to test this model further.

C-Nap1 forms a ringlike assembly at the proximal end of both centrioles (Fig. 8*B*). C-Nap1 organizes two types of rootletin/CEP68

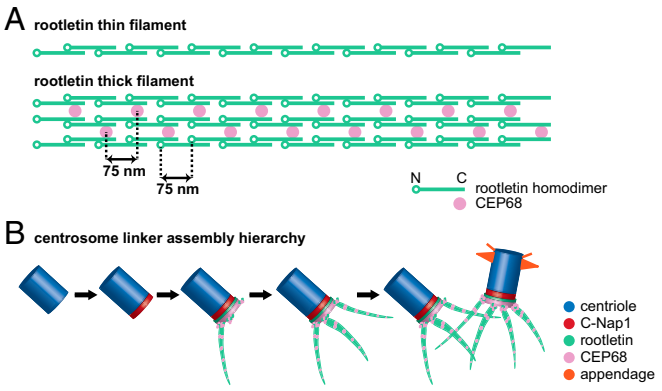

Fig. 8. Model. (*A*) Rootletin filament assembly with and without CEP68. (*B*) Assembly hierarchy of centrosome linker C-Nap1, CEP68, and rootletin at centrosomes. See text for details.

structures: first, a rootletin ring that surrounds the centriole; and second, filaments as described earlier that originate from the rootletin ring (Fig. 8*B*). The precise structure of the rootletin ring surrounding centrioles is still unclear. It could be composed of short rootletin filaments, or rootletin molecules may have a radial orientation around centrioles similar to what has been observed for PCNT, of which the C terminus is close to centrioles and the N terminus more distant (3). CEP68 depletion mainly affected the outward-radiating rootletin filaments but also affected, to a lower degree, the rootletin pool close to C-Nap1, indicating different CEP68 requirements. Rootletin directly binds to C-Nap1 (20), explaining why the structural integrity of the C-Nap1 pool of rootletin was less dependent on CEP68. Rootletin/CEP68 dots on the centriole ring likely function as nucleation seeds or anchoring points for the assembly of filaments. However, similar to tubulin and G-actin that use nucleators in cells but can also shelf-assemble into polymers when the concentration is high enough (31, 32), rootletin assembles into cytoplasmic filaments without the aid of C-Nap1 and CEP68 when overexpressed (this study and refs. 8 and 9).

How do rootletin/CEP68 filaments connect the two interphase centrosomes of a cell? The STED microscopy and 3D-STORM data suggest that rootletin/CEP68 filaments coming from different centrosomes are interwoven into a web-like structure (Fig. 8*B*). Moreover, live-cell imaging analysis has shown that the centrosome linker is a flexible structure that can lose and regain linker function without the disassembly of centrosome linker filaments (Movies S4–S6). In addition, centrosome linkage can be overcome by microtubule motor forces provided by the kinesin-5 motor Eg5 (33). These data together are most consistent with a model of flexible interweaved rootletin/CEP68 filaments that form regional contacts. However, presently, we cannot exclude the possibility that a single centrosome-to-centrosome fiber can also provide linkage function. The extended web-like centrosome linker potentially has the properties of forming a landing platform for signaling molecules. In addition, it may function as contact sites for cytoskeletal elements with yet unappreciated functions.

Materials and Methods

For all STED data, except Fig. 3 *A* and *B*; Fig. 4*A*, *Middle* and *Bottom*; Fig. 5*B*, siCEP68; *SI Appendix*, Figs. S3 and S4 *A–C*; and the corresponding *SI Appendix*, Fig. S11 (here we used an Abberior Instruments 775 STED), we used a home-built STED microscope similar to the one published in ref. 23 with a 594- and 650-nm excitation laser combined with a 775-nm STED laser (*SI Appendix*, Fig. S12). The STED images were, unless specified differently, corrected for background (ImageJ background subtraction with a rolling ball radius of 30 to 50 pixels), followed by resampling to half the pixel size (10 nm) and Wiener deconvolution with point-spread functions of 27 to 40 nm and 190 to 250 nm. Due to the large spread in intensities, to show all features, linear background subtraction and intensity scaling was applied. All raw data are shown in *SI Appendix*, Fig. S11, and an overview of the measured cell is given in *SI Appendix*, Table S1.

Details are in *SI Appendix*, *Details of Materials and Methods*, including experimental procedures and reagents.

No animal or clinical experiments were performed. HUVECs were obtained from A. Fischer, German Cancer Research Center, Heidelberg, with the approval of the Medical Ethics Commission of the Medical Faculty Mannheim, Heidelberg University (S-175/2015).

ACKNOWLEDGMENTS. We thank Dr. E. Nigg (Biozentrum, University of Basel) for CEP68 and C-Nap1 antibodies; Dr. J. Pines (Gurdon Institute) for providing Flp-In T-Rex RPE1 cells; Dr. A. Fischer (German Cancer Research Center) for HUVECs; Dr. A. Fry (University of Leicester) for pEGFP-rootletin plasmid; Dr. M. Pagano (New York University) for pcDNA3-FLAG-CEP68 plasmid; and Ursula Jaekle for technical support. This work is supported by Deutsche Forschungsgemeinschaft Grant Schi295/6-1 (to E.S.), Netherlands Organisation for Scientific Research Grant 680-50-1501 (to R.V.), and European Molecular Biology Organization Grant ALTF 1516-2015 (to R.V.).

1. Nigg EA, Stearns T (2011) The centrosome cycle: Centriole biogenesis, duplication and inherent asymmetries. *Nat Cell Biol* 13:1154–1160.
2. Bettencourt-Dias M, Glover DM (2007) Centrosome biogenesis and function: Centrosomics brings new understanding. *Nat Rev Mol Cell Biol* 8:451–463.
3. Lawo S, Hasegan M, Gupta GD, Pelletier L (2012) Subdiffraction imaging of centrosomes reveals higher-order organizational features of pericentriolar material. *Nat Cell Biol* 14:1148–1158.
4. Agircan FG, Schiebel E, Mardin BR (2014) Separate to operate: Control of centrosome positioning and separation. *Philos Trans R Soc Lond B Biol Sci* 369:20130461.
5. Fry AM, et al. (1998) C-Nap1, a novel centrosomal coiled-coil protein and candidate substrate of the cell cycle-regulated protein kinase Nek2. *J Cell Biol* 141:1563–1574.
6. Bahe S, Stierhof YD, Wilkinson CJ, Leiss F, Nigg EA (2005) Rootletin forms centriole-associated filaments and functions in centrosome cohesion. *J Cell Biol* 171:27–33.
7. Graser S, Stierhof YD, Nigg EA (2007) Cep68 and Cep215 (Cdk5rap2) are required for centrosome cohesion. *J Cell Sci* 120:4321–4331.
8. Yang J, et al. (2002) Rootletin, a novel coiled-coil protein, is a structural component of the ciliary rootlet. *J Cell Biol* 159:431–440.
9. Akiyama T, et al. (2017) SHG-specificity of cellular rootletin filaments enables naïve imaging with universal conservation. *Sci Rep* 7:39967.
10. Potter C, et al. (2017) Multiple isoforms of Nesprin1 are integral components of ciliary rootlets. *Curr Biol* 27:2014–2022.e6.
11. He R, et al. (2013) LRRC45 is a centrosome linker component required for centrosome cohesion. *Cell Reports* 4:1100–1107.
12. Fang G, et al. (2014) Centlein mediates an interaction between C-Nap1 and Cep68 to maintain centrosome cohesion. *J Cell Sci* 127:1631–1639.
13. Faragher AJ, Fry AM (2003) Nek2A kinase stimulates centrosome disjunction and is required for formation of bipolar mitotic spindles. *Mol Biol Cell* 14:2876–2889.
14. Mardin BR, et al. (2013) EGF-induced centrosome separation promotes mitotic progression and cell survival. *Dev Cell* 25:229–240.
15. Kaseda K, McAinsh AD, Cross RA (2012) Dual pathway spindle assembly increases both the speed and the fidelity of mitosis. *Biol Open* 1:12–18.
16. Nam HJ, van Deursen JM (2014) Cyclin B2 and p53 control proper timing of centrosome separation. *Nat Cell Biol* 16:538–549.
17. Panic M, Hata S, Neuner A, Schiebel E (2015) The centrosomal linker and microtubules provide dual levels of spatial coordination of centrosomes. *PLoS Genet* 11:e1005243.
18. Mazo G, Soplop N, Wang WJ, Uryu K, Tsou MF (2016) Spatial control of primary ciliogenesis by subdistal appendages alters sensation-associated properties of cilia. *Dev Cell* 39:424–437.
19. Floriot S, et al. (2015) C-Nap1 mutation affects centriole cohesion and is associated with a Seckel-like syndrome in cattle. *Nat Commun* 6:6894.
20. Yang J, Adamian M, Li T (2006) Rootletin interacts with C-Nap1 and may function as a physical linker between the pair of centrioles/basal bodies in cells. *Mol Biol Cell* 17:1033–1040.
21. Hell SW, Wichmann J (1994) Breaking the diffraction resolution limit by stimulated emission: Stimulated-emission-depletion fluorescence microscopy. *Opt Lett* 19:780–782.
22. Hell SW (2007) Far-field optical nanoscopy. *Science* 316:1153–1158.
23. Görlitz F, et al. (2014) A STED microscope designed for routine biomedical applications. *Prog Electromagnetics Res* 147:57–68.
24. Venkataramani V, Herrmannsdörfer F, Heilemann M, Kuner T (2016) SuReSim: Simulating localization microscopy experiments from ground truth models. *Nat Methods* 13:319–321.
25. Rust MJ, Bates M, Zhuang X (2006) Sub-diffraction-limit imaging by stochastic optical reconstruction microscopy (STORM). *Nat Methods* 3:793–795.
26. Bock H, et al. (2007) Two-color far-field fluorescence nanoscopy based on photoswitchable emitters. *Appl Phys B* 88:161–165.
27. Liao H, Winkfein RJ, Mack G, Rattner JB, Yen TJ (1995) CENP-F is a protein of the nuclear matrix that assembles onto kinetochores at late G2 and is rapidly degraded after mitosis. *J Cell Biol* 130:507–518.
28. Sonnen KF, Schermelleh L, Leonhardt H, Nigg EA (2012) 3D-structured illumination microscopy provides novel insight into architecture of human centrosomes. *Biol Open* 1:965–976.
29. Mennella V, et al. (2012) Subdiffraction-resolution fluorescence microscopy reveals a domain of the centrosome critical for pericentriolar material organization. *Nat Cell Biol* 14:1159–1168.
30. Djinovic-Carugo K, Gautel M, Ylänne J, Young P (2002) The spectrin repeat: A structural platform for cytoskeletal protein assemblies. *FEBS Lett* 513:119–123.
31. Kollman JM, et al. (2015) Ring closure activates yeast γTuRC for species-specific microtubule nucleation. *Nat Struct Mol Biol* 22:132–137.
32. Firat-Karalar EN, Welch MD (2011) New mechanisms and functions of actin nucleation. *Curr Opin Cell Biol* 23:4–13.
33. Mardin BR, et al. (2010) Components of the Hippo pathway cooperate with Nek2 kinase to regulate centrosome disjunction. *Nat Cell Biol* 12:1166–1176.
34. Fava LL, et al. (2017) The PIDDosome activates p53 in response to supernumerary centrosomes. *Genes Dev* 31:34–45.